version April 29, 2014: fm
Preprint typeset using LaTeX style emulateapj v. 04/17/13

SLAC-PUB-15872

THE LOW-FREQUENCY RADIO CATALOG OF FLAT SPECTRUM SOURCES

F. Massaro[1,2], M. Giroletti[3], R. D'Abrusco[4], N. Masetti[5], A. Paggi[4],
Philip S. Cowperthwaite[4], G. Tosti[6] & S. Funk[2].

version April 29, 2014: fm

ABSTRACT

A well known property of the γ-ray sources detected by COS-B in the 1970s, by the Compton Gamma-ray Observatory in the 1990s and recently by the *Fermi* observations is the presence of radio counterparts, in particular for those associated to extragalactic objects. This observational evidence is the basis of the radio-γ-ray connection established for the class of active galactic nuclei known as blazars. In particular, the main spectral property of the radio counterparts associated with γ-ray blazars is that they show a flat spectrum in the GHz frequency range. Our recent analysis dedicated to search blazar-like candidates as potential counterparts for the unidentified γ-ray sources (UGSs) allowed us to extend the radio-γ-ray connection in the MHz regime. We also showed that below 1 GHz blazars maintain flat radio spectra. Thus on the basis of these new results, we assembled a low-frequency radio catalog of flat spectrum sources built by combining the radio observations of the Westerbork Northern Sky Survey (WENSS) and of the Westerbork in the southern hemisphere (WISH) catalog with those of the NRAO Very Large Array Sky survey (NVSS). This could be used in the future to search for new, unknown blazar-like counterparts of the γ-ray sources. First we found NVSS counterparts of WSRT radio sources and then we selected flat spectrum radio sources according to a new spectral criterion specifically defined for radio observations performed below 1 GHz. We also described the main properties of the catalog listing 28358 radio sources and their logN-logS distributions. Finally a comparison with with the Green Bank 6-cm radio source catalog has been performed to investigate the spectral shape of the low-frequency flat spectrum radio sources at higher frequencies.

Subject headings: galaxies: active - quasars: general - surveys - radiation mechanisms: non-thermal

1. INTRODUCTION

Since the epoch of the first γ-ray observations performed by COS-B in the 1970s (e.g., Hermsen et al. 1977) and by the Compton Gamma-ray Observatory in the 1990s (e.g., Hartman et al. 1999), a link between the radio and the γ-ray sky was discovered. It has been used to associate the high-energy sources with their low-energy counterparts (e.g. Mattox et al. 1997). This radio-to-γ-ray relation has also been recently highlighted for the extragalactic sources detected by the *Fermi* mission (Atwood et al. 2009). In particular, **nearly** all the γ-ray sources associated in the second *Fermi* Large Area Telescope (LAT) catalog (2FGL; Nolan et al. 2012) and/or in the second catalog of active galactic nuclei (AGNs) (Ackermann et al. 2011a) detected by the *Fermi*-LAT have a clear radio counterpart. This is the basis of the radio-γ-ray connection specifically discussed for blazars (e.g., Ghirlanda et al. 2010; Mahony et al. 2010; Ackermann et al. 2011b), that constitute the rarest class of AGNs (e.g., Urry & Padovani 1995; Massaro et al. 2009; Massaro et al. 2011a) and the largest known population of γ-ray sources (e.g., Abdo et al. 2010).

Recently we addressed the problem of searching for γ-ray blazar candidates as counterparts of the unidentified γ-ray sources (UGSs) adopting a new approach that employs the low-frequency radio observations performed by the Westerbork Synthesis Radio Telescope (WSRT). While performing this investigation we found that the radio-γ-ray connection of blazars can be extended below $\sim$1 GHz (Massaro et al. 2013a).

Our analysis was based on the combination of the radio observations from Westerbork Northern Sky Survey (WENSS; Rengelink et al. 1997) at 325 MHz with those of the NRAO Very Large Array Sky survey (NVSS; Condon et al. 1998) and of the Very Large Array Faint Images of the Radio Sky at Twenty-Centimeters (FIRST; Becker et al. 1995; White et al. 1997) at about 1.4 GHz. A similar analysis was also performed using the Westerbork in the southern hemisphere (WISH) survey (De Breuck et al. 2002) at 352 MHz (Nori et al. 2014). Both of these studies were based on the observational evidence that blazars also show flat radio spectra below $\sim$1 GHz (see also Kovalev 2009a; Kovalev et al. 2009b; Petrov et al. 2013, for recent analyses).

The flatness of the blazar radio spectra is a well known property expected from radio data in the GHz frequency range (e.g., Ivezíc et al. 2002; Healey et al. 2007; Kimball & Izević 2008, for recent

[1] SLAC National Laboratory and Kavli Institute for Particle Astrophysics and Cosmology, 2575 Sand Hill Road, Menlo Park, CA 94025, USA
[2] Yale Center for Astronomy and Astrophysics, Physics Department, Yale University, PO Box 208120, New Haven, CT 06520-8120, USA
[3] INAF Istituto di Radioastronomia, via Gobetti 101, 40129, Bologna, Italy
[4] Harvard - Smithsonian Astrophysical Observatory, 60 Garden Street, Cambridge, MA 02138, USA
[5] INAF - Istituto di Astrofisica Spaziale e Fisica Cosmica di Bologna, via Gobetti 101, 40129, Bologna, Italy
[6] Dipartimento di Fisica, Università degli Studi di Perugia, 06123 Perugia, Italy

Work supported in part by US Department of Energy under contract DE-AC02-76SF00515.

analyses). This spectral property was also used in the past for the associations of γ-ray sources since the EGRET era (e.g., Mattox et al. 1997). However, despite a small survey of BL Lac objects at 102 MHz (Artyukh & Vetukhnovskaya 1981), the low radio frequency spectral behavior of blazars was still an unexplored region of the electromagnetic spectrum until our recent analyses (Massaro et al. 2013a; Nori et al. 2014). Using WSRT data at 325 MHz and at 352 MHz as well as those of very low-frequency observations of the Very Large Array Low-Frequency Sky Survey[7] (VLSS; Cohen et al. 2007) at 74 MHz we showed that blazars maintain a flat radio spectrum even below ∼100 MHz and we extended the radio-γ-ray connection below ∼1 GHz (Massaro et al. 2013b).

Thus, motivated by these recent results we assembled a catalog of low-frequency flat spectrum radio sources using the combination of both the WENSS and the WISH surveys with the NVSS. The main aim of this investigation is to provide the counterpart, at longer wavelengths, of the Combined Radio All-Sky Targeted Eight-GHz Survey (CRATES) used to associate *Fermi* objects with blazar-like sources (Healey et al. 2007).

The paper is organized as follows: in Section 2 we briefly present the main properties of the low-frequency radio survey performed by WSRT and used to carry out our investigation (i.e., the WENSS and the WISH). In Section 3 we search for the NVSS counterparts of WSRT sources. Then in Section 4 we extract the main low-frequency catalog of flat spectrum radio sources (LORCAT) from the combined WSRT-NVSS surveys and we discuss on its main properties. Section 5 is devoted to the comparison the Green Bank 6-cm (GB6) radio source catalog (e.g., Gregory et al. 1996) to investigate the spectral behavior of LORCAT sources at higher frequencies. Finally, Section 6 is dedicated to the summary and the conclusions.

For our numerical results, we use cgs units unless stated otherwise Spectral indices, α, are defined by flux density, $S_\nu \propto \nu^{-\alpha}$. The WSRT catalogs used to carry out our analysis are available from both the HEASARC[8,9] and the VIZIER[10,11] databases as well as that of the NVSS[12,13].

2. WESTERBORK LOW-FREQUENCY RADIO SURVEY

The Westerbork Northern Sky Survey (WENSS) is a low-frequency radio survey that covers the northern sky above +30° in declination performed at 325 MHz to a limiting flux density of ∼18 mJy at 5 sigma level (Rengelink et al. 1997). The version of the WENSS catalog used in our analysis was implemented as a combination of two separate catalogs obtained from the WENSS Website[14]: the WENSS Polar Catalog that comprises 18186 sources above +72° in declination and the WENSS Main Catalog including 211234 objects in the declination range between +28° and +76°.

We also used the Westerbork In the Southern Hemisphere (WISH) catalog[15] that is the southern extension of the WENSS. WISH is a low-frequency (352 MHz) radio survey covering most of the sky between -26°and -9° at 352 MHz to the same limiting flux density of the WENSS. It is worth noticing that the Galactic Plane region at galactic latitudes $|b|$ <10° are excluded from the WISH observations. Due to the very low elevation of the observations, the survey has a much lower resolution in declination than in right ascension. A correlation with the NVSS shows that the positional accuracy is less constrained in declination than in right ascension, but there is no significant systematic error (see De Breuck et al. 2002, for more details). Finally, we highlight that the WISH catalog contains multiple observations of the same source for many objects as well as measurements of individual components of multi-component sources.

3. RADIO SPATIAL ASSOCIATIONS

We adopted the following statistical approach to find the radio NVSS counterparts at 1.4 GHz for the sources in the WSRT low radio frequency surveys, namely: the WENSS and the WISH.

For each radio source listed in either the WENSS and the WISH surveys, we searched for all the NVSS counterparts that lie within elliptical regions that corresponds to the positional uncertainty at 95% level of confidence (i.e., 2σ). We took into account the uncertainties on both the right ascension, α, and the declination, δ, in the WSRT and in the NVSS surveys.

We found that the total number of correspondences is 225933 out of 268425 radio sources included in either the WSRT surveys. We excluded from our analysis all the WSRT source with radio analysis flags **(i.e., P and Y as reported in the WENSS and WISH catalog, respectively, to indicate that there were problems in the model fitting for a source)** and variability flag in the WISH observations, all the double matches and all those sources labeled as components of a multi-component source (flag "C") in the WSRT catalogs. In addition, for this version of the LORCAT catalog, we also excluded from our sample 2707 multiple matches since their WSRT radio flux densities could be due to the emission of several, unresolved, NVSS sources so contaminating our estimates of the low frequency spectral index.

We then built 100 mock realizations of the WSRT catalog by shifting each source position in a random direction of the sky by a fixed length of 1°. This shift adopted to create the mock WSRT catalogs were chosen not too distant from the original WSRT position and within the NVSS footprint so to obtain fake catalogs with a sky distribution similar to the original WSRT and to perform the cross-match with each fake catalog and the NVSS taking into account the local density distribution of the WSRT radio sources. The total number of WSRT sources in each mock realization is also preserved.

For each mock realization of the WSRT catalog, we counted the number of associations with the NVSS occurring at angular separations R smaller than 300″. Then we computed the mean number $\lambda(R)$ of these mock asso-

[7] http://lwa.nrl.navy.mil/VLSS/
[8] WENSS:http://heasarc.gsfc.nasa.gov/W3Browse/all/wenss.html
[9] WISH: http://heasarc.gsfc.nasa.gov/W3Browse/all/wish.html
[10] WENSS: http://vizier.u-strasbg.fr/viz-bin/VizieR?-source=VIII/62
[11] WISH: http://cdsarc.u-strasbg.fr/viz-bin/Cat?VIII/69A
[12] http://heasarc.gsfc.nasa.gov/W3Browse/all/nvss.html
[13] http://vizier.u-strasbg.fr/viz-bin/VizieR?-source=%20NVSS
[14] http://www.astron.nl/wow/testcode.php?survey=1
[15] http://www.astron.nl/wow/testcode.php?survey=2

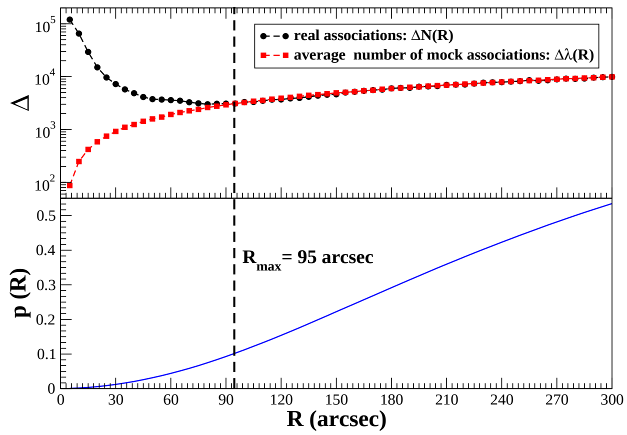

FIG. 1.— Upper panel) The values of $\Delta\,\lambda(R)$ (red circles) and $\Delta\,N(R)$ (black squares) as function of the angular separation R. Our choice of R_{max} is marked by the vertical dashed line. It occurs at the first R value for which $\Delta\,\lambda(R) \simeq \Delta\,N(R)$. Lower panel) The probability of having spurious associations $p(R)$ as function of the angular separation R.

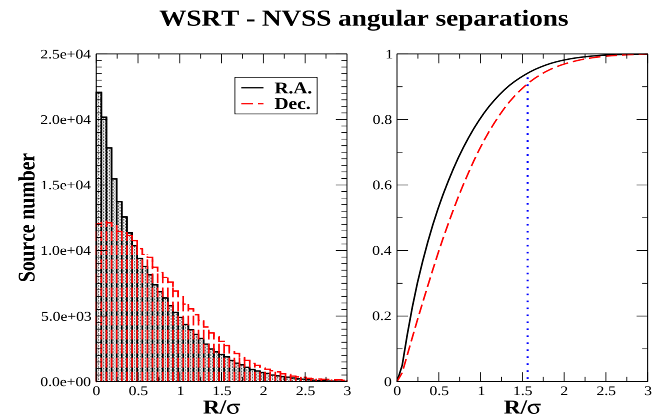

FIG. 2.— Left panel) The distributions of ratio between angular separations R and the positional uncertainties for the right ascension (black straight line) and for the declination (red dashed line), respectively for the selected 224438 WSRT - NVSS radio sources. Right panel) The cumulative distribution of the ratio R/σ. The dotted blue line marks the 90% limit (see also Section 3).

ciations, averaged over the 100 fake WSRT catalogs and verifying that $\lambda(R)$ has a Poissonian distribution. Increasing the radius by $\Delta\,R$ =5″, we also computed the difference $\Delta\,\lambda(R)$ as:

$$\Delta\,\lambda(R) = \lambda(R + \Delta\,R) - \lambda(R)\,, \qquad (1)$$

In Figure 1 we show the comparison between $\Delta\,N(R)$ and $\Delta\,\lambda(R)$. For radii larger than R_{max} =95″the $\Delta\,\lambda(R)$ curve superimposes that of $\Delta\,N(R)$ indicating that WSRT-NVSS cross-matches could occur by chance at angular separations larger than R_{max}. Thus we choose R_{max} as to the maximum angular separation between the WSRT and the NVSS position to consider the 1.4GHz radio source a reliable counterpart of a WSRT object.

In addition we calculated the chance probability of spurious associations $p(R)$ as the ratio between the number of real associations $N(R)$ and the average of those found in the mock realizations of the WSRT catalog $\lambda(R)$, corresponding to a value of $\sim$10% for $R = R_{max}$ (see e.g., Maselli et al. 2010; Massaro et al. 2011b; D'Abrusco et al. 2013; Massaro et al. 2013c, for a similar procedure to estimate the probability of spurious associations).

We then computed the uncertainties on the WSRT positions according to the procedure described in Rengelink et al. (1997) and combined them with the NVSS ones (Condon et al. 1998) using the following relation:

$$\sigma_{RA,Dec} = \sqrt{\sigma^2_{RA,Dec}(WSRT) + \sigma^2_{RA,Dec}(NVSS)}, \quad (2)$$

We also defined the angular separation normalized to the values of the positional uncertainties m as:

$$m = \sqrt{\left(\frac{R_{RA}}{\sigma_{RA}}\right)^2 + \left(\frac{R_{Dec}}{\sigma_{Dec}}\right)^2} \qquad (3)$$

where R_{RA} and R_{DEC} are the angular separations in right ascension and in declination, respectively.

In Figure 2 we show the distributions of the ratio between the angular separation R and the combined positional uncertainty σ for RA and Dec, respectively. In order to build the final sample of WSRT - NVSS correspondences that will be used to extract the low-frequency radio catalog of flat spectrum sources, we selected only sources with $m < 3$. This WSRT - NVSS final sample lists 224438 radio sources out of 225933 previously selected. We note that we found a potential NVSS counterpart for about 85% of the WSRT sources, and since we adopted a threshold on m =3, this corresponds to a completeness C of about 80%, evaluated according to the relations described in Condon et al. (1975). Moreover, this is also in agreement with the reliability of our associations, estimated via Monte Carlo simulations, occurring at R_{max} that is of the order to 10% (see Figure 1).

4. LOW-FREQUENCY RADIO CATALOG OF FLAT SPECTRUM SOURCES

4.1. *Radio spectral index distribution at low-frequencies*

For the WSRT-NVSS associations we defined a low-frequency radio spectral index: α_{low}, using the integrated flux densities at 325 MHz from the WENSS and those at 352 MHz reported in the WISH, S_{325} and S_{352}, respectively, in combination with the NVSS S_{1400} at 1.4 GHz as:

$$\alpha_{low} = -k_1 \cdot log(S_{1400}/S_{low})\;, \qquad (4)$$

where the k_1 factor is equal to 1.58 and 1.67 (i.e., $[log(1400/325)]^{-1}$ and $[log(1400/352)]^{-1}$) for the WENSS and the WISH surveys, respectively, S_{low} is the flux density at 325 MHz (WENSS) or at 352 MHz (WISH) with all flux densities in units of mJy. The uncertainties on α_{low} where computed according to the following relation:

$$\sigma_{low} = k_2 \cdot \sqrt{(\sigma_{1400}/S_{1400})^2 + (\sigma_{low}/S_{low})^2} \qquad (5)$$

where the k_2 factor is equal to 0.68 and 0.72 (i.e., $\mid [ln(1400/325)]^{-1} \mid$ and $\mid [ln(1400/352)]^{-1} \mid$) for the

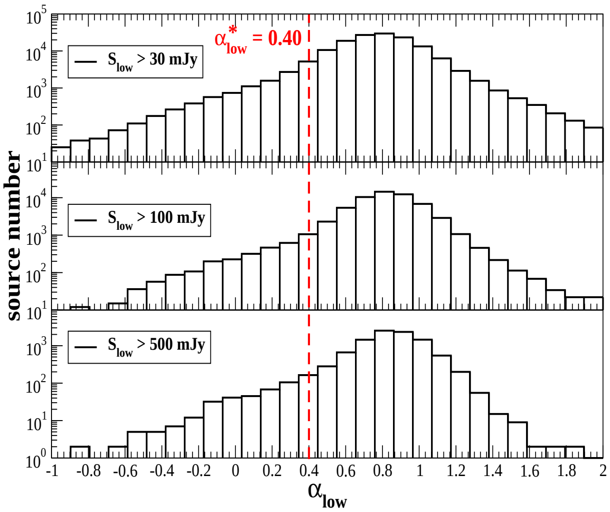

FIG. 3.— The distributions of α_{low} for three flux limited subsamples extracted from the WSRT-NVSS correspondences. Flux density cuts are reported in each panel. It is clear how the distribution has a tail for low values of the low-frequency spectral index but it does not appear to have a bimodal shape as in previous radio analyses at higher frequencies (see e.g., Witzel et al. 1979; Owen et al. 1983; Condon et al. 1984a; Condon et al. 1989). The red dashed line marks our threshold to define low-frequency flat spectrum radio sources at α_{low}=0.4.

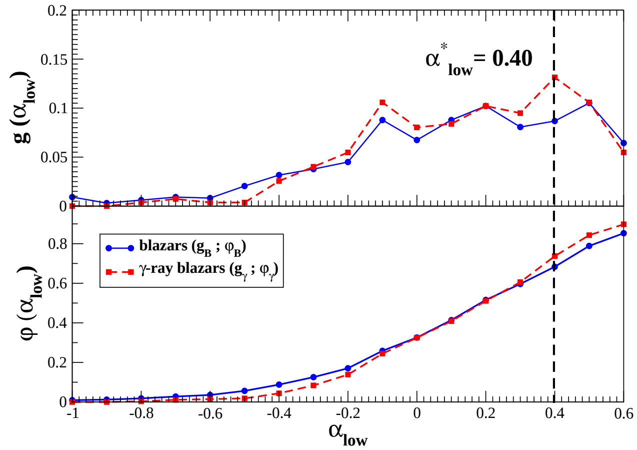

FIG. 4.— Upper panel) The fractional efficiency $g(\alpha_{low})$ defined by Eq. 7 for blazars (blue line), the subsample of *Fermi* blazars (red line) all with α_{low} between -1 and 0.7 (dashed black line). Lower panel) The completeness ϕ defined as the ratio between the total number of sources with ($\alpha_{low} < \alpha^*_{low}$) and the total number of expected sources, computed for blazars (blue line), the *Fermi* blazars (red line; see Section 4.1 for more details). The chosen threshold α^*_{low} =0.4, adopted to create the LORCAT, is highlighted by the dashed vertical line in both panels.

WENSS and the WISH surveys, respectively while σ_{1400} and σ_{low} are the uncertainties on the WSRT and NVSS flux densities.

In radio astronomy it is conventional to indicate flat spectrum radio sources as those with a two-point spectral index $\alpha(\nu_1,\nu_2)$ ∼0 or typically lower than 0.5 (e.g. Condon et al. 1984a). The origin of these thresholds reside in the distribution of the two-point spectral indices measured between ∼1.4 GHz and ∼5 GHz for a number of flux-limited source samples (Witzel et al. 1979; Owen et al. 1983; Condon et al. 1984a; Condon et al. 1989). As shown in these analyses, the (unnormalized) spectral-index distributions consist of a narrow steep-spectrum component with $\alpha(\nu_1,\nu_2)$ ∼0.7 and a broader flat-spectrum component centered on $\alpha(\nu_1,\nu_2)$ ∼0. As the sample selection frequency is lowered, the number of steep-spectrum sources increases rapidly and the median spectral indices of both components increase (e.g., Kellermann 1974; Condon et al. 1989). As reported by Kellermann et al. (1964), the increase in $\alpha(\nu_1,\nu_2)$ of each spectral component is proportional to the square of its width, so the median spectral index of the flat-spectrum component changes more rapidly with frequency.

As shown in Figure 3, even considering three or more flux limited subsample of the WSRT-NVSS associated sources, we were not able to identify a bimodal behavior in the spectral index distribution of α_{low}. This, in addition to the frequency dependence highlighted by Kellerman (1964), suggest that a different criterion has to be chosen to indicate flat spectrum radio sources at low frequencies.

We noticed that both blazars and *Fermi* blazars detected in the WENSS show values of α_{low} between -1 and 0.65 for the largest fraction of their samples (Massaro et al. 2013a). Specifically, in our previous analysis we considered low-frequency flat spectrum radio sources as those having α_{low} <0.65. This occurred for 90% of the blazars detected by *Fermi* and for more than 80% of those listed in the ROMA-BZCAT (Massaro et al. 2009; Massaro et al. 2011a). However, to assemble the LORCAT, we adopted a more conservative threshold based on the following statistical criterion.

First we established the number of blazars and *Fermi* blazars that we expect to find within this subsample simply performing the crossmatch with the ROMA-BZCAT within 8″.5 as adopted in our previous analysis. We found that the number of expected blazars with a WSRT counterpart is 979, including 274 *Fermi* blazars. For a given value of the threshold α^*_{low}, we defined the fractional efficiency $g(\alpha_{low})$ as the ratio between the difference of total number of sources having: $\alpha_{low} < \alpha^*_{low}$ and those with $(\alpha_{low} - \Delta\,\alpha) < \alpha^*_{low}$ and the total number of expected sources N_{exp} within the WSRT-NVSS associations with -1< α_{low} <0.7:

$$g(\alpha_{low}) = \frac{N(\alpha_{low} < \alpha^*_{low}) - N((\alpha_{low} - \Delta\,\alpha) < \alpha^*_{low})}{N_{exp}} \tag{6}$$

where $\Delta\,\alpha$= 0.1. In particular, $g(\alpha_{low})$ has been computed for all blazars (i.e., $g_B(\alpha_{low})$), the subsample of *Fermi* blazars (i.e., $g_\gamma(\alpha_{low})$) with -1< α_{low} <0.7 (see Figure 4). Since the main goal underlying the LORCAT is to have a catalog of potential counterparts for the UGSs, we chose the α^*_{low} =0.4 threshold as the value corresponding to the peak of the $g_\gamma(\alpha_{low})$. According to the above threshold the total number of low-frequency sources with a flat radio spectrum listed in the LORCAT is 28358 having -1< α_{low} <0.40. **Adopting the**

above criterion on the choice of the α_{low}threshold the LORCAT catalog will be less complete. However, the selected low frequency flat spectrum radio sources are more reliable to be γ-ray blazar candidates since this criterion ensures to avoid the heavy contamination by steep spectrum radio sources.

In Figure 4 we also show the completeness φ of the sample considered above defined as the ratio between the total number of sources with Our criterion is then supported by the comparison at high-frequency described in Section 5. ($\alpha_{low} < \alpha^*_{low}$) and the total number of expected sources:

$$\varphi(\alpha_{low}) = \frac{N(\alpha_{low} < \alpha^*_{low})}{N_{exp}} \quad (7)$$

Thus we noticed that for our choice of α^*_{low} =0.4 we are able to re-associate 80% of the *Fermi* blazars of all blazars listed in the WSRT-NVSS with α_{low} between -1 and 0.65 (Massaro et al. 2013a).

In Table 1 we listed all LORCAT sources with their WSRT and NVSS names. For all these sources we also report the NVSS coordinates, the angular separation R between the NVSS and the WSRT positions, the α_{low} value with its uncertainty σ_{low} and the WSRT survey name which each original source belong to: WISH or WENSS.

Finally, we note that, as found by our previous analysis (e.g., Massaro et al. 2013a), the source density of the LORCAT sources is ∼1.8 src/deg^2, given the total 4.7 sr of footprint of the combined WENSS-WISH survey (3.1 sr in the WENSS plus 1.6 sr in the WISH) while according to the ROMA-BZCAT the blazar density is currently of the order of 0.1 src/deg^2. So we can expect that only about 10% of the sources in the LORCAT are blazar-like, however, to confirm this insight optical spectroscopic observations and high frequency radio data are necessary. **Moreover,** since the ROMA-BZCAT is not a survey and it is not a complete catalog, the above estimate on the expected fraction of blazars present in the LORCAT has to be considered carefully.

4.2. *Flux density distributions at low-frequencies*

Comparing the radio flux densities at 1.4 GHz S_{1400} and at low frequencies S_{low} (i.e., 325 for the WENSS and 352 MHz for the WISH), as shown in Figure 5, there is a good match between the two WSRT and NVSS observations: bright sources below ∼1 GHz tend to be among the brightest also above 1 GHz. In Figure 5 we also report the line corresponding to a radio spectrum of α_{low}=0. Then in Figure 6, we also compare the low-frequency radio spectral index α_{low} with the archival WSRT and NVSS flux densities. The logN-logS distribution for all of the WSRT-NVSS associations per range of low-frequency spectral indices between -1 and 1.5 as well as that of our LORCAT are reported in Figure 7. Then Figure 8 shows the logN-logS distributions for the LORCAT sample for both the WSRT and the NVSS flux densities. These logN-logS distributions are in agreement with the evolution of the radio source counts (e.g., Condon et al. 1984b; Condon et al. 1998). These logN-logS distributions computed with both the S_{low} and S_{1400} for all the LORCAT sources appear to

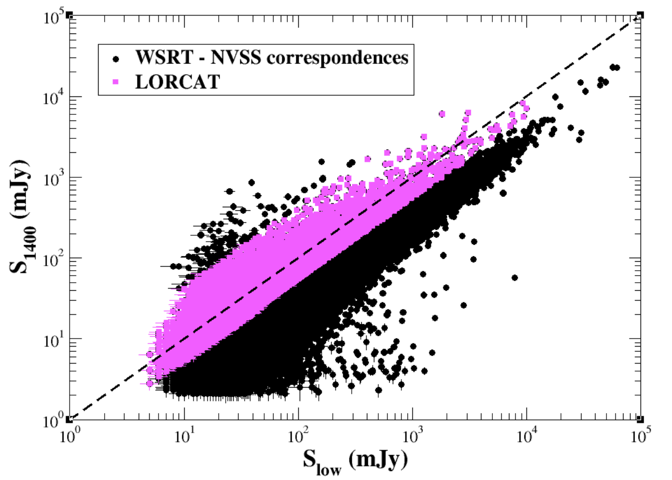

Fig. 5.— The flux density scatterplot. LORCAT sources (magenta circles) are shown in comparison with those associated in the whole WSRT-NVSS crossmatch (black circles). The dashed black line marks the radio spectral index α_{low} =0.

have the same shape. This is expected as the flux densities are mildly correlated, as shown in Figure 5. In Figure 8 we also show the $N \propto S^{-1.5}$ line expected in the case of a uniform source distribution at not too large redshift (i.e. in a Euclidean universe). It is well know that blazars show a broken luminosity function due to the relativistic effects of their beamed emission (e.g. Urry & Shafer 1984), this could be also reflected in the logN-logS distribution in agreement with that of the LORCAT. However to prove this effect redshift estimates will be necessary for these low-frequency sources with flat radio spectra.

5. COMPARISON WITH THE GREEN BANK 6-CM RADIO SOURCE CATALOG

A detailed identification of the complete LORCAT sample is out of the scope of the present analysis and in particular a multifrequency analysis of the optical and the IR counterparts of the LORCAT sources will be presented in a separate, forthcoming paper (Massaro et al. 2014 in prep.). However to understand the nature of the selected low-frequency flat spectrum radio sources we performed a crossmatch with the Green Bank 6-cm radio source catalog (GB6)[16] (Gregory et al. 1996) to investigate the spectral properties of the LORCAT sources at ∼5 GHz.

It is worth noting that among all the radio surveys at frequency grater than ∼1 GHz the GB6 is the most recent one covering the largest portion of the LORCAT footprint since it was performed between 0° and +75° in declination. The GB6 radio source catalog is also complete above 50 mJy (Gregory et al. 1996). Since the CRATES catalog have been compiled using the GB6 in the above range of declination, a comparison with it is nested within the following analysis.

The total number of LORCAT sources within the GB6 footprint is 15814. Assuming the difference $\Delta\alpha$ (i.e., $\Delta\alpha = \alpha_{high} - \alpha_{low}$) between the low (i.e., α_{low}) and the high-frequency (i.e., α_{high}) spectral indices equal to zero with α_{high} defined as -1.85$\cdot log(S_{4850}/S_{1400})$, we com-

[16] http://heasarc.gsfc.nasa.gov/W3Browse/all/gb6.html

TABLE 1
LORCAT Main Table (first 10 lines).

WSRT name	NVSS name	R.A. (NVSS) (J2000)	Dec. (NVSS) (J2000)	R arcsec	α_{low}	σ_{low}	survey
0000.0+3323	J000238+334008	00:02:38.41	+33:40:08.3	6.27	0.18	0.12	wenss
0000.0+4449	J000237+450554	00:02:37.65	+45:05:54.1	10.98	0.38	0.1	wenss
0000.0+5005	J000236+502220	00:02:36.82	+50:22:20.3	6.78	-0.28	0.12	wenss
0000.0+6737	J000235+675422	00:02:35.79	+67:54:22.7	2.78	0.33	0.07	wenss
0000.0-1838	J000239-182128	00:02:39.71	-18:21:28.8	29.83	0.28	0.16	wish
0000.1+4452	J000244+450928	00:02:44.17	+45:09:28.5	4.39	0.07	0.08	wenss
0000.1+4628	J000242+464509	00:02:42.71	+46:45:09.0	10.26	0.0	0.09	wenss
0000.2-2131	J000249-211419	00:02:49.81	-21:14:19.3	4.43	-0.15	0.03	wish
0000.2-2251	J000250-223437	00:02:50.77	-22:34:37.7	9.52	0.29	0.14	wish
0000.3+2926	J000252+294253	00:02:52.36	+29:42:53.2	3.15	0.22	0.06	wenss

Col. (1) WSRT name.
Col. (2) NVSS counterpart of the WSRT source.
Col. (3) R.A. from the NVSS catalog.
Col. (4) Dec. from the NVSS catalog.
Col. (5) Angular separation between the WSRT and the NVSS position: R.
Col. (6) Low frequency radio spectral index α_{low}.
Col. (7) Uncertainty on the α_{low}.
Col. (8) WSRT original survey: WENSS or WISH.

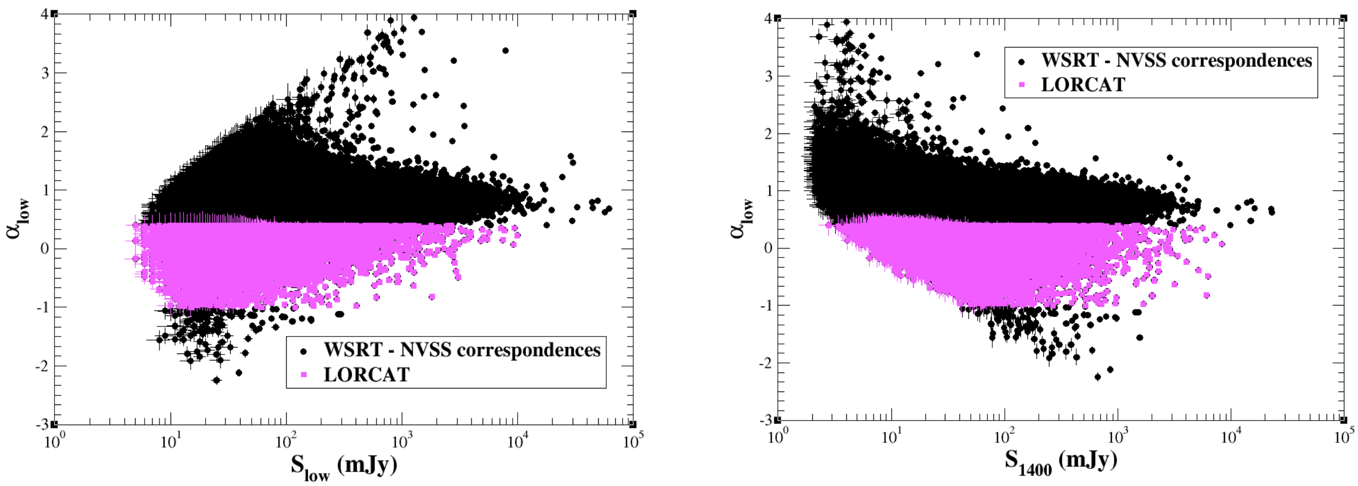

Fig. 6.— *Left panel*) The scatterplot of the low-frequency spectral index α_{low} with respect to the WSRT flux density. *Right panel*) The same scatter plot where the NVSS flux density is reported on the x axis.

puted the extrapolated flux density at 4.85 GHz $S_{ex,4850}$ for the LORCAT sources to determine those expected to be detected in the GB6. We found that above the completeness threshold of the GB6, there are 3219 LORCAT sources having $S_{ex,4850}$ >50mJy.

Then searching the correspondences between the LORCAT and the GB6 catalogs, we found 1942 out of the 3219 (i.e., ∼60%) are detected at 6-cm within their positional uncertainty regions at 1σ level of confidence, computed between the NVSS and the GB6 positions. In particular only 875 out of these 1942 radio sources show a flux density S_{4850} above the completeness limit of the GB6 survey. The distribution of the high-frequency spectral index α_{high} computed with the observed S_{4850} in the GB6 for the 2834 LORCAT-GB6 associations is reported in Figure 9 together with their $\Delta\alpha$ histogram. More than ∼75% of the 1942 LORCAT sources detected in the GB6 still have a "flat" radio spectrum at frequencies above ∼1 GHz (see Figure 9), according to the canonical, widely accepted definition of flat spectrum radio sources (i.e., α_{high} <0.5) (e.g., Kellermann 1974; Condon et al. 1989, and references therein). This strongly support our definition of low-frequency "flat" radio spectra (see Section 4.1). However, a significant fraction (i.e., ∼60%)of these GB6-LORCAT sources appear to have radio spectra that steepens toward higher frequencies (i.e., $\Delta\alpha >$ 0).

In particular, it is worth mentioning that the subclass of BZQs generally show flat high-frequency spectra, thus LORCAT sources with steep high-frequency spectra may not actually be BZQs (e.g., Condon et al. 1983). However, $\Delta\alpha$ > 0 is occurring for a small fraction (i.e., ∼5%) of the known blazars listed in the ROMA-BZCATand these are all classified as BL Lac objects. In Figure 10 we also report the radio spectral index α_{843}^{1400} evaluated for all the ROMA-BZCAT blazars that have radio observations in the NVSS and in the Sydney University Molonglo Sky Survey (SUMSS; Mauch et al. 2003) at 843 MHz. It is evident that blazars show a clear steepening a higher frequencies in agreement with that found for the LORCAT sources. In addition, there could also be the possibility that these radio spectra are intrinsically mildly curved (e.g., Howard et al. 1965; Kellermann et al. 1969; Pauliny-Toth et al. 1972). It is known that spectral curvature appears at higher frequencies in the sub millimeter data (e.g., Giommi et al. 2007; Giommi et al. 2012).

Finally, we note the presence of radio sources with

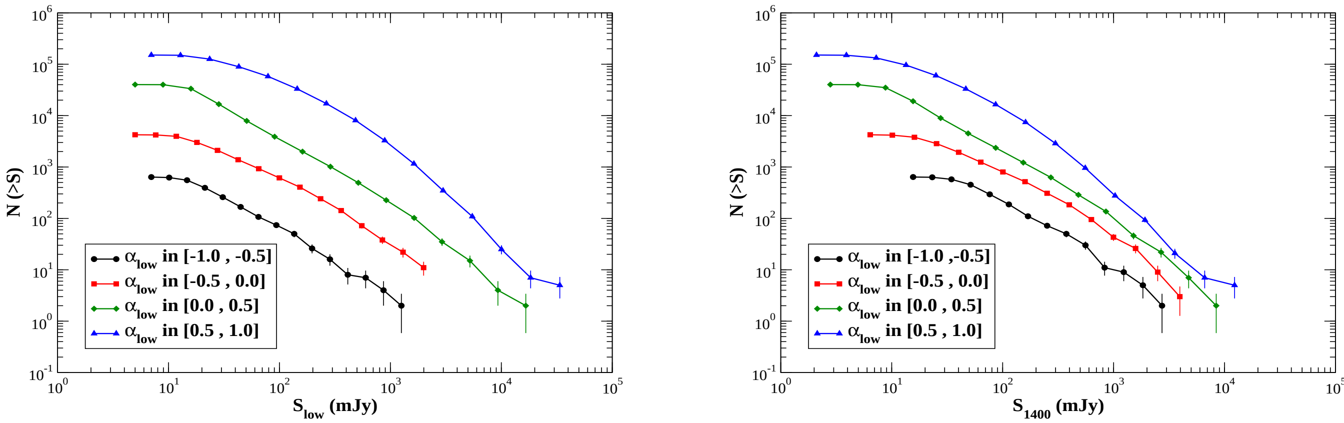

FIG. 7.— *Left panel*) The logN-logS distributions evaluated for all the WSRT-NVSS correspondences with the low-frequency flux density S_{low} for different range of α_{low} between the values -1 and 1. *Right panel*) Same as the left panel for the logN-logS distributions computed using the NVSS flux densities at 1.4 GHz.

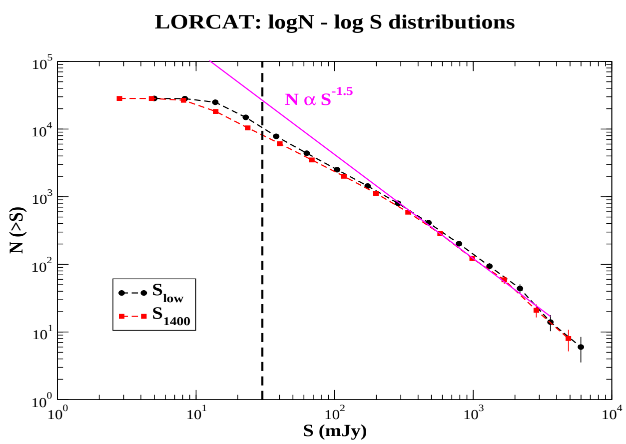

FIG. 8.— The logN-logS distributions of the LORCAT sample calculated with the WSRT flux density S_{low} (black circles) and with that of the NVSS at 1.4 GHz (red squares). A similar shape for the two logN-logS distributions of the LORCAT sample is expected since the S_{low} and S_{1400} flux densities are correlated (see Figure 5). The magenta line indicates the $N \propto S^{-1.5}$ relation expected from a uniform source distribution, while the vertical dashed black line marks the completeness limit of the WSRT survey at 30 mJy.

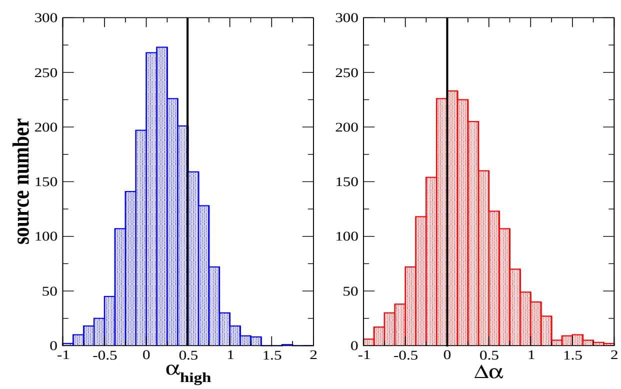

FIG. 9.— Left panel) The distribution of the high-frequency spectral index α_{high} computed for all the LORCAT sources with a counterpart in the GB6 survey within their radio positional uncertainties (see Section 5 for more details). It is worth noting that a significant fraction of sources having flat spectra at low frequencies between ∼300 MHz and ∼1 GHz (i.e., $-1 < \alpha_{low} < 0.4$) appear to be relatively flat, according to the general definition (i.e., $\alpha_{high} < 0.5$ marked by the vertical black line), also at high frequencies between ∼1 GHz and ∼5 GHz. Right panel) The distribution of the $\Delta\alpha = \alpha_{high} - \alpha_{low}$ for the LORCAT-GB6 radio correspondences. Radio sources with flatter high-frequency spectrum with respect to the low-energy one have $\Delta\alpha < 0$ while those steepening at high frequencies show $\Delta\alpha > 0$. The vertical dashed line marks the threshold Δα=0.

$\Delta\alpha < 0$ in the LORCAT sources might indicate that the low-frequency emission could be contaminated by that of extended components. These cannot be resolved with the large beam of the low-frequency survey and in general present steep spectra (see e.g., Massaro et al. 2013b, for a recent discussion).

6. SUMMARY AND CONCLUSIONS

We have assembled a low-frequency radio catalog of flat spectrum sources (LORCAT) built by combining the radio observations of the two main WSRT surveys (i.e., WENSS and WISH) at 325 MHz and 352 MHz, respectively, with those of the NVSS at 1.4 GHz. The main goals underlying the creation of this catalog are similar to those of the CRATES (Healey et al. 2007) since both can be used in the future to search for new, unknown blazar-like counterparts of the γ-ray sources [17].

We defined a new criterion to associate WSRT and NVSS sources improving our previous analyses (Massaro et al. 2013a; Nori et al. 2014) and we provided a new definition of flat spectrum radio sources at low-frequencies based on the distribution of the spectral index α_{low} between 325 MHz and 1.4 GHz found for blazars in the ROMA-BZCAT. Sources with radio analysis flags as well as double matches between the radio surveys have been excluded from our final list. Thus the

[17] The LORCAT catalog has been already used for the γ-ray source associations that will be released with the the next *Fermi* catalog actually in preparation.

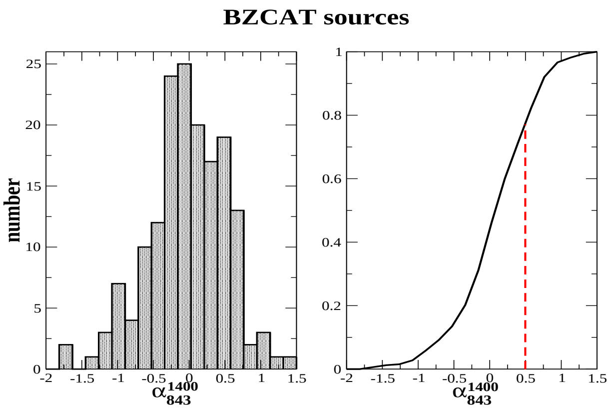

FIG. 10.— The distribution of the radio spectral index α_{843}^{1400} for all the known blazars that lie within the NVSS and in the SUMSS footprints (left panel). The cumulative distribution is shown on the right panel where the red dashed line marks the α_{843}^{1400} =0.5, according to the canonical definition of flat spectrum radio sources.

LORCAT sample comprises 28358 radio sources including ∼667 known blazars having $-1 < \alpha_{low} < 0.4$.

Then we also compared our LORCAT catalog with the the Green Bank 6-cm (GB6) radio catalog, since it is the most recent radio survey covering the largest fraction of the LORCAT footprint at higher frequency (i.e., ∼5 GHz). We found that a significant fraction of the LORCAT sources with extrapolated flux densities at ∼5 GHz above the completeness threshold of the GB6 are detected (i.e., ∼86%). In addition they also appear to be "flat" spectrum radio sources above ∼1 GHz, according to the canonical definition (i.e., α_{high} <0.5) (e.g., Condon et al. 1989, and references therein). The lack of detections for a small fraction of the LORCAT sources in the GB6 footprint could be explained in terms of a spectral steeping toward high frequencies (i.e., a mild curvature) as already observed in blazars.

Finally, we highlight that to investigate the nature of the LORCAT sources, aiming to identify the fraction of γ-ray blazar candidates associable to *Fermi* sources, a detailed analysis of the IR and optical properties is necessary. It will be presented in a separate, forthcoming paper (Massaro et al. 2014 in prep.).

We are in debt with our anonymous referee for many helpful comments and for all the checks performed on our tables. This work is supported by the NASA grants NNX12AO97G and NNX13AP20G. R. D'Abrusco gratefully acknowledges the financial support of the US Virtual Astronomical Observatory, which is sponsored by the National Science Foundation and the National Aeronautics and Space Administration. The work by G. Tosti is supported by the ASI/INAF contract I/005/12/0. P.S.C. is grateful for support from the NSF through the NSF Graduate Research Fellowships Program Grant DGE1144152 The WENSS project was a collaboration between the Netherlands Foundation for Research in Astronomy and the Leiden Observatory. We acknowledge the WENSS team consisted of Ger de Bruyn, Yuan Tang, Roeland Rengelink, George Miley, Huub Rottgering, Malcolm Bremer, Martin Bremer, Wim Brouw, Ernst Raimond and David Fullagar for the extensive work aimed at producing the WENSS catalog. Part of this work is based on archival data, software or on-line services provided by the ASI Science Data Center. This research has made use of data obtained from the high-energy Astrophysics Science Archive Research Center (HEASARC) provided by NASA's Goddard Space Flight Center; the SIMBAD database operated at CDS, Strasbourg, France; the NASA/IPAC Extragalactic Database (NED) operated by the Jet Propulsion Laboratory, California Institute of Technology, under contract with the National Aeronautics and Space Administration. Part of this work is based on the NVSS (NRAO VLA Sky Survey): The National Radio Astronomy Observatory is operated by Associated Universities, Inc., under contract with the National Science Foundation. TOPCAT[18] (Taylor 2005) for the preparation and manipulation of the tabular data and the images.

Facilities:WSRT, VLA, GBT.

REFERENCES

Abdo, A. A. et al. 2010 ApJS 188 405
Abdo, A. A. et al. 2014a ApJS in prep.
Abdo, A. A. et al. 2014b ApJS in prep.
Ackermann, M. et al. 2011a ApJ, 743, 171
Ackermann, M. et al. 2011b ApJ, 741, 30
Ackermann, M., et al. 2012, Science, 338, 1190
Artyukh, V. S.& Vetukhnovskaya, Y. N. 1981 SvA, 25, 397
Atwood, W. B. et al. 2009 ApJ, 697, 1071
Becker, R. H. et al. 1995 ApJ, 450, 559
Cohen, A. S. et al. 2007 AJ, 134, 1245
Condon, J.J. et al. 1975 AJ, 80, 887
Condon, J. J. et al. 1983, AJ, 88, 20
Condon, J.J. 1984a ApJ, 287, 461
Condon, J.J. 1984b ApJ, 284, 44
Condon J. J. 1988 "Galactic and Extragalactic Radio Astronomy" 2nd edition, eds. G.L. Verschuur and K.I. Kellermann
Condon J. J. 1989 ApJ, 338, 13
Condon, J. J. et al.1998, AJ, 115, 1693
D'Abrusco, R. et al. 2012 ApJ, 748, 68
D'Abrusco, R. et al. 2013 ApJS, 206, 12
De Breuck, C. et al. 2002 A&A, 394, 59
Ghirlanda, G. et al. 2010 MNRAS, 407, 791
Giommi, P. et al. 2007 A&A, 468, 571
Giommi, P. et al. 2012 A&A, 541A, 160
Gregory, P. C. et al. 1996 ApJS, 103, 427
Hartman, R.C. et al. 1999 ApJS, 123, 79
Healey, S. E. et al. 2007 ApJS, 171, 61
Hermsen, W. et al. 1977 Natur, 269, 494
Howard, William E., III et al. 1965 ApJS, 10, 331
Kellermann, K.I. 1964 ApJ 140, 969
Kellermann, K. I. et al. 1969 ApJ, 157, 1
Kellermann, K.I. 1974 "Galactic and Extragalactic Radio Astronomy" eds. G.L. Verschuur and K.I. Kellermann
Kimball, A. & Izević, Z. 2008 AJ, 136, 684
Kovalev, Y. Y. 2009 ApJ, 707L, 56
Kovalev, Y. Y. et al. 2009 ApJ, 696L, 17
Ivezić, Z. et al. 2002 AJ, 124, 2364
Mahony, E. K. et al. 2010 ApJ, 718, 587
Maselli, A. et al. 2010 A&A, 512A, 74
Massaro, E. et al. 2009 A&A, 495, 691
Massaro, E. et al. 2011a "Multifrequency Catalogue of Blazars (3rd Edition)", ARACNE Editrice, Rome, Italy
Massaro, F. et al. 2011b ApJ, 740L, 48
Massaro, F. et al. 2012b ApJ, 752, 61
Massaro, F. et al. 2013a ApJS, 207, 4
Massaro, F. et al. 2013b ApJS, 208, 15

[18] http://www.star.bris.ac.uk/∼mbt/topcat/

Massaro, F. et al. 2013c ApJS, 206, 13
Massaro, F. et al. 2013d ApJS, 209, 10
Massaro, F. et al. 2014 ApJS in prep.
Mattox, J. R. et al. 1997 Apj, 481,95
Mauch, T. et al. 2003 MNRAS, 342, 1117
Nolan et al. 2012 ApJS, 199, 31
Nori, M., Giroletti, M., Massaro, F., D'Abrusco, R., Paggi, A. & Tosti, G. et al. 2014 ApJS 212, 3
Owen, F.N., J.J. Condon & J.E. Ledden. 1983. AJ, 88, 1
Pauliny-Toth, I. I. K. et al. 1972 AJ, 77, 265
Petrov, L. et al. 2013 MNRAS, 432, 1294
Rengelink, R. et al. 1997, A&A Suppl. 124, 259
Taylor M. B., 2005, ASPC, 347, 29
Urry, C. M., & Shafer, R. A. 1984 ApJ, 280, 569
Urry, C. M., & Padovani, P. 1995 PASP, 107, 803
White, R. L. et al. 1997 ApJ, 475, 479
Witzel, A. et al. 1979 AJ. 84, 942.